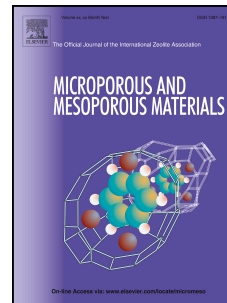# Accepted Manuscript

On the Zeolitic Imidazolate Framework-8 (ZIF-8) Membrane for Hydrogen Separation from Simulated Biomass-derived Syngas

Hang Yin, Taehee Lee, Dr. Jungkyu Choi, Dr. Alex C.K. Yip

Please cite this article as: H. Yin, T. Lee, J. Choi, A.C.K. Yip, On the Zeolitic Imidazolate Framework-8 (ZIF-8) Membrane for Hydrogen Separation from Simulated Biomass-derived Syngas, *Microporous and Mesoporous Materials* (2015), doi: 10.1016/j.micromeso.2015.10.033.

This is a PDF file of an unedited manuscript that has been accepted for publication. As a service to our customers we are providing this early version of the manuscript. The manuscript will undergo copyediting, typesetting, and review of the resulting proof before it is published in its final form. Please note that during the production process errors may be discovered which could affect the content, and all legal disclaimers that apply to the journal pertain.

Graphical Abstract
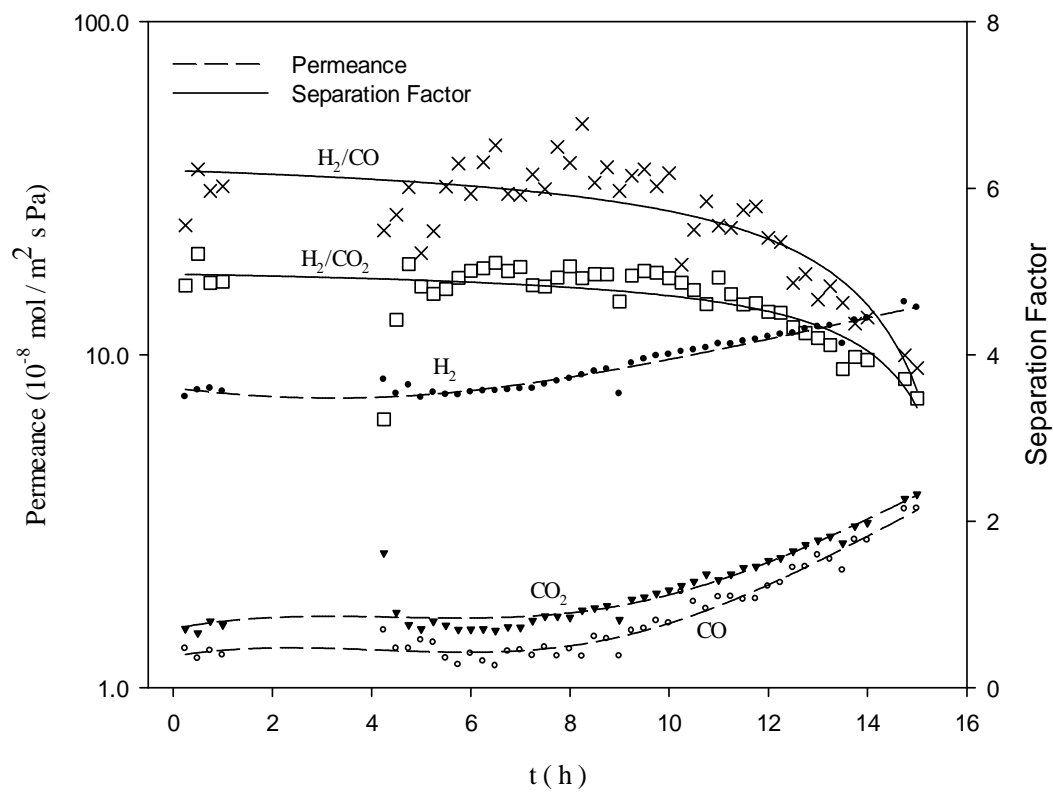
On the Zeolitic Imidazolate Framework-8 (ZIF-8) Membrane for Hydrogen Separation from Simulated Biomass-derived Syngas

Hang Yin,[a] Taehee Lee,[b] Jungkyu Choi,[b,c,*] Alex C. K. Yip[a,**]

[a] Department of Chemical and Process Engineering, University of Canterbury, Christchurch, New Zealand

[b] Department of Chemical and Biological Engineering, Korea University, Seoul, Republic of Korea

[c] Green School, Korea University, Seoul, Republic of Korea

Corresponding authors:

* Dr. Jungkyu Choi, Department of Chemical and Biological Engineering & Green School, Korea University, Republic of Korea. Tel: +82 2 32904854; Fax: +82 2 9266102.
Email address: jungkyu_choi@korea.ac.kr

** Dr. Alex C.K. Yip, Department of Chemical and Process Engineering, University of Canterbury, Christchurch, New Zealand. Tel: +64 3 364-2534; Fax: +64 3 364-2063.
Email address: alex.yip@canterbury.ac.nz

Abstract

Hydrogen separation from biomass-derived syngas is a critical step in the utilization of gasification technology. Compared with the traditional methods, membrane technology provides an effective and low-cost solution for adjusting the gas composition and collecting H_2 in syngas environments. In this study, a zeolitic imidazolate framework-8 (ZIF-8)-based membrane, which is a potential candidate for H_2 separation from biomass-derived syngas, was successfully fabricated through the seeded (secondary) growth method and the subsequent post-treatments. The prepared ZIF-8 membrane exhibited a modest H_2 separation performance for H_2/CO_2 and H_2/CO, with separation factors of 4.95 and 6.08, respectively, and a H_2 permeance of 7.81×10^{-8} $mol \cdot m^{-2} \cdot s^{-1} \cdot Pa^{-1}$ at 200 °C in the simulated biomass-derived syngas environments ($H_2/CO_2/CO$) with the presence of steam. In particular, the H_2/CO_2 and H_2/CO separation factors were increased by 36% and 97%, respectively, with respect to those obtained through bare supports. Despite the promising H_2 perm-selectivity, the H_2/CO_2 and H_2/CO separation factors of ZIF-8 membranes at 200 °C under water-containing syngas environments were maintained up to 10 h but the longer exposure led to the gradual degradation and eventual reduction toward those of bare supports after 15 h seemingly due to the water-involved membrane degradation. This study provides the availability and limitation of ZIF-8 membranes for H_2 separations in stimulated biomass-derived syngas environments.

1. Introduction

Biomass is an environmentally friendly renewable energy source that is widely considered as a promising alternative for fossil fuel. Gasification is one of the most attractive biomass conversion technologies for the production of valuable energy products from multiform biomass feedstocks. The primary product of gasification is the producer gas or syngas, which mainly contains hydrogen, carbon monoxide, carbon dioxide, and water vapor. Biomass–derived syngas can be used for power generation, synthesis of Fisher-Tropsch liquid fuel, and other forms of energy after further chemical transformations [1-4]. It is noted that the control of the H_2/CO molar ratio and the production of concentrated H_2 are highly desirable for effective utilization of the syngas [5, 6]. New Zealand has abundant biomass resources, including woody waste, agricultural waste, and other commercial crops. Hence, biomass conversion is a promising energy option for New Zealand [7, 8]. In this aspect, a dual fluidized bed (DFB) steam gasifier has been developed as means to produce syngas from biomass resources effectively [1, 3, 4]. In this study, we aim to use the membrane-based separation, which is a promising gas separation technology compared to other traditional methods [9, 10], to produce concentrated H_2 stream in this biomass-derived syngas system.

As a member of metal organic frameworks (MOFs), zeolitic imidazolate frameworks (ZIFs) are novel emerging porous materials composed of divalent metal nodes linked by imidazolate bridging ligands [11-16]. ZIF materials are regarded as "zeolitic" because their 145° metal-imidazolate-metal angles are very close to the zeolite Si–O–Si angle [14, 17-21]. In addition to the general property advantages of most MOF materials, such as the adjustable pore

3

size and the high surface area, ZIFs have high chemical and thermal stability [14, 22, 23]. Over 150 ZIF structures have been developed by incorporating different metals and functional ligand groups, which has resulted in a variety of zeolite-like topologies and special chemical functionalities.

The structural robustness and other advantages make ZIFs promising materials in many application areas, including separation and adsorption [22, 24-26], catalysis [27-30], and drug delivery [31]. Among these applications, the most promising utilizations of ZIFs are in separation membranes [32-36] and selective sorbents [37]. For example, a supported ZIF-7 membrane was prepared in Caro's group for hydrogen separation and exhibited separation factors of 13.6 for H_2/N_2 and 18 for H_2/CO_2 [32]. A ZIF-8 membrane was fabricated in aqueous solution and was successfully employed to separate a propylene/propane mixture by Lai's group [38]. In addition, a counter-diffusion method was employed for the facile synthesis of ZIF-8 membranes, which showed good propylene/propane separation performance [39]. A 3-aminopropyltriethoxysilane (APTES)-modified ZIF-90 membrane was developed by Huang et al. with a CO_2/CH_4 separation factor of 4.7, which is promising in the application of CO_2/CH_4 separation [40].

ZIF-8 membrane synthesis methods have been investigated and developed under different conditions for many separation applications. In particular, ZIF-8 has a relatively high chemical and thermal stability compared to other MOFs [14]. The pore size of ZIF-8 (~0.34 nm), which is larger than the kinetic diameter of H_2 (0.289 nm) and CO_2 (0.33 nm), but smaller than CO (0.376 nm), N_2 (0.364 nm), and CH_4 (0.38 nm) [41], allows it to be used potentially for gas separation

4

processes in industry [42]. Although the pore size of ZIF-8 is slightly larger than the kinetic diameter of CO_2, ZIF-8 membranes were expected to separate H_2/CO_2 mixtures through the recognition of their size difference [43]. However, modest H_2/CO_2 separation performance has been reported [24, 26, 42, 44], requiring a substantial work on understanding the structural properties of ZIF-8 membranes and thus, improving their separation performances. There are two primary classifications of the synthesis methods; in situ growth [26, 34] and secondary growth [25, 33, 35]. Some innovative procedures have also been developed [45]. The effects of other features in ZIF-8 membrane synthesis have been discussed, including the substrate effect, the solvent effect, and the activation procedure effect. This information has been summarized by Melgar et al. [46] and Pimentel et al [22].

Herein, a ZIF-8 membrane is considered an alternative solution for separating hydrogen from biomass-derived syngas. Although many investigations have focused on ZIF-8 membrane fabrication and development, the complex mechanisms of ZIF membrane formation cause difficulties in the reproducible control of the outstanding performance of the synthesized ZIF-8 membrane. A well-integrated ZIF-8 membrane often requires many synthesis attempts because of the unstable performance of the synthesized membranes. In addition, despite the promising potential of ZIF-8 membranes for H_2 separations and the reported excellent stability of ZIF-8 material, the hydrothermal stability of ZIF-8 membranes remains uncertain under the application conditions, especially in biomass-derived syngas environments with the presence of steam. In this study, a post-treatment procedure was proposed to provide a simple, feasible way to improve the ZIF-8 membrane fabrication process and repair the imperfect ZIF-8 membrane. Moreover, the gas permeation performance of the post-treated ZIF-8 membrane was examined by single gas

permeation at room temperature and mixture gas permeation at different temperatures in a simulated biomass-derived syngas environment both with and without the presence of steam. To the best our knowledge, the hydrothermal stability of the ZIF-8 membrane was for the first time studied via a long-term operation under simulated humid syngas environments at 200 °C.

2. Experimental

2.1. Materials

Zinc chloride (99.9%) was purchased from Ajax Chemicals. Zinc nitrate hydrate (>99.99%), 2-methyimidazole (Hmim), methanol (>99.8%), and sodium formate were purchased from Sigma-Aldrich Chemical Co. All chemicals were used as received without further treatment. For permeation tests, instrument-grade hydrogen, nitrogen, argon, carbon dioxide, carbon monoxide, and a simulated biomass-derived syngas with a gas composition of 50 vol% H_2, 25 vol% CO and 25 vol% CO_2 were purchased from BOC. Deionized (DI) water was produced in a lab-based reverse osmosis water treatment plant.

2.2. ZIF-8 membrane fabrication and post-treatment

2.2.1. Seed synthesis

Nano-sized ZIF-8 crystals were synthesized according to the method of Cravillon et al [18]. In general, 0.386 g $Zn(NO_3)_2 \cdot 6H_2O$ and 0.4175 g Hmim were dissolved in 25 ml methanol. The Hmim solution was then added to the Zn solution with stirring for 30 min at room temperature. The mixture was then aged under a static condition for 24 h to form the colloidal

ZIF-8 seeds. The solid crystals were collected by centrifuge and were washed with methanol 3 times. Subsequently, the ZIF-8 seeds were dried in a vacuum oven at 50 °C overnight. Finally, a 0.1 wt% seeding solution was obtained by dispersing the ZIF-8 powder in methanol under ultrasonication.

2.2.2. Membrane fabrication

A porous α-alumina disc support of 3 mm thickness and 22 mm diameter was prepared by hydraulic pressing followed by programmed temperature calcination. Prior to being seeded, the support was polished with fine sandpaper to obtain a smooth seeding surface and was then washed in an ultrasonic water bath. After the support was dried at 120 °C, it was dip-coated in the prepared seed solution for 10 seconds 2 times and dried in an oven at 80 °C overnight.

The secondary growth solution was prepared according to the method reported by Bux et al [24]. In detail, 0.5460 g $ZnCl_2$, 0.2781 g $NaHCO_2$, and 0.4698 g Hmim were dissolved in 40 ml methanol under ultrasonication for 1 min and were then stirred for 5 min. The clear solution was carefully poured into a Teflon-lined autoclave with the seeded support loaded vertically. The autoclave was treated in an oven at 120 °C for 6 h. After the autoclave was cooled to room temperature, the membrane was removed and washed with methanol. Finally, the membrane was dried at room temperature for 24 h.

2.2.3. Post-treatment of the imperfect membrane

The dried ZIF-8 membrane was considered an imperfect membrane if it did not have a reasonable H_2/N_2 ideal selectivity in the single gas permeation test. Then, post-treatment was performed in the following two steps to refine the membrane. First, the imperfect membrane was gently polished to smooth the membrane surface with fine sandpaper (#1600). If it was still an imperfect membrane after the polishing treatment, then the following 2nd step was carried out. The membrane surface was further polished to deliberately break the top thin layer of the ZIF-8 membrane into small ZIF-8 particles, re-generating a uniform ZIF-8 seeded support layer. Subsequently, a 2nd membrane synthesis was conducted by repeating the procedures in section 2.2.2 and the polishing post-treatment followed. This post-treatment procedure is similar to a method that Tao et al. reported [35].

2.3. Gas permeation test and characterization

A single gas permeation test was conducted by using the system, shown in Fig. 1a, at room temperature, and a mixture gas permeation test was performed by using the Wicke-Kallenbach system, shown in Fig. 1b, at different temperatures. The membrane was loaded into a permeation cell sealed with a silicon o-ring and was then activated under argon flow before testing. In the mixture gas permeation test, the feed gas flow rate was 30 ml/min and the total pressure (approximately 3 atm) at the feed/retentate side was controlled using a needle valve. In the permeate side, argon was used as the sweep gas to dilute the gas concentration and the total pressure was maintained at 1 atm. The gas compositions of the retentate and the permeate streams were analyzed with a gas chromatograph (Buck scientific 910 GC) configured with both a thermal conductivity detector (TCD) and a flame ionization detector (FID) equipped with a

methanizer. An Agilent ADM 2000 flow meter was used to measure the flow rate in both tests. Scanning electron microscopy (SEM) was performed on a JEOL 700F. X-ray diffraction (XRD) patterns of the samples were collected using a Philips PW1700 instrument equipped with a Co Kα radiation source. The separation factor, $\alpha_{i/j}$ for the gas mixtures was calculated from equation (1):

$$\alpha_{i/j} = \frac{y_i/y_j}{x_i/x_j} \tag{1}$$

where x_i and x_j represent the mole fraction of species i and j in the feed side, while y_i and y_j represent the mole fraction of species i and j in the permeate side.

3. Results and Discussion

3.1. ZIF-8 membrane synthesis and post-treatment

The average size of the synthesized ZIF-8 seeds was approximately 100 nm with a uniform size distribution, as shown in Fig. 2a. Fig. 2b and c show the top surface of the support before and after the seeding procedure, indicating that the support is uniformly covered by the ZIF-8 seeds after the double dip-coating procedure. The single gas permeation results at room temperature are summarized in Table. 1. The bare support exhibited a pure gas H_2 permeance of 11.5×10^{-6} mol·m^{-2}·s^{-1}·Pa^{-1} and H_2/CO_2, H_2/CO, and H_2/N_2 ideal selectivities of 3.63, 3.08, and 3.02, respectively. These ideal selectivities suggest that gas permeation through the bare support followed the combined mechanisms of Knudsen diffusion and laminar flow [47]. Although the gas permeances of the imperfect ZIF-8 membrane decreased more than 10 times after the membrane synthesis procedure, the ideal selectivities of H_2/CO_2 and H_2/N_2 were not improved

compared with the bare support but rather decreased to 3.03 and 2.59, respectively. The top surface and cross-section SEM images of the imperfect ZIF-8 membrane are shown in Fig. 2d and 2e, respectively. Although a well-integrated membrane layer was likely to be formed on the top of the support, the membrane surface was very bumpy and uneven apparently due to the formation of large ZIF-8 crystals with an average particle size over 20 µm. Fig. 2d and e reveal that these disordered large ZIF-8 crystals are randomly cross-linked and spread throughout the support, and the membrane thickness is over 40 µm. After polishing the surface of the imperfect ZIF-8 membrane, all of the gas permeances were significantly decreased and in particular, the H_2 permeance was reduced to 20.5×10^{-8} $mol \cdot m^{-2} \cdot s^{-1} \cdot Pa^{-1}$, which was 3 times lower than that of the imperfect ZIF-8 membrane. Compared to the above-mentioned imperfect ZIF-8 membranes, the H_2/CO_2, H_2/CO, and H_2/N_2 ideal selectivities were improved to 4.79, 8.87, and 13.06, respectively, which were comparable to other reports [46]. It was found that the ideal selectivity of H_2/N_2 was higher than that of H_2/CO, though the kinetic diameter of CO (0.376 nm) was larger than that of N_2 (0.364 nm). The lower H_2/CO ideal selectivity can be ascribed to the stronger CO adsorption compared with weak N_2 adsorption on the ZIF-8 surface [37]. Fig. 2f shows that the top surface of the 1st polished ZIF-8 membrane was flatter and that the edges of the large ZIF-8 crystals were polished away. At the same time, some debris particles were observed on the polished membrane surface, which were likely to be the broken ZIF-8 fragments. The cross-section image of the 1st polished ZIF-8 membrane, shown in Fig. 2g, demonstrates that the ZIF-8 membrane layer exhibited a reduced thickness of *ca* 20 µm after the polishing post-treatment.

The schematic diagram shown in Fig. 3 is proposed to explain the effects of the polishing post-treatment. As shown in Fig. 3a, before the polishing treatment, the rough surface of the imperfect ZIF-8 membrane could result in a defective contact area between the membrane surface and the sealing o-ring, possibly generating an undesired shortcut for the permeating gas molecules. Rather than passing along the ZIF-8 membrane thickness to the permeate side, it is easier for the pressurized gas molecules to flow through the defects due to the incomplete sealing, where the transport resistance is smaller. Accordingly, the ZIF-8 membrane failed to achieve the gas separation performance, as expected by the molecular sieve effect. Thus, it resulted in the low ideal selectivities of H_2/CO_2 and H_2/N_2, as reflected by the single gas permeation results of the imperfect ZIF-8 membrane (Table 1). In contrast, the polishing post-treatment procedure could eliminate or at least reduce significantly the sealing defects, allowing for the formation of a flat membrane top layer, as shown in Fig. 3b. Under this circumstance, the feed gas can be effectively sieved by the ZIF-8 membrane, improving the perm-selectivity of hydrogen over larger molecular gases.

Despite the definite improvement via the polishing post-treatment, careful and precise control is required during this manual polishing process. If the membrane layer is damaged by excessive polishing, it would result in poor H_2 separation performance again. For this case, the 2nd time synthesis was conducted in this study in an attempt to repair the membrane for reliable membrane-based H_2 separations. The single gas permeation results obtained through the ZIF-8 membrane after 2nd time synthesis and polishing are also listed in Table 1. The single gas permeances and the corresponding ideal selectivities of the membrane after the 2nd time synthesis and polishing are comparable to those of the 1st polished membrane. It appears that a polishing of

the imperfect ZIF-8 membrane prior to the 2nd time synthesis produced ZIF-8 seeds effectively by fragmenting the membrane constituents [35]. In the industrial manufacture perspective, this additional seeded growth (i.e., tertiary growth) is highly desirable, since this post-treatment method can reduce the membrane manufacturing cost via repairing membranes that show poor separation performance.

In addition, Fig. 4 shows the XRD patterns of the ZIF-8 membranes before and after the post-treatments along with those of ZIF-8 seeds and the simulated XRD patterns of ZIF-8 and α-alumina. At this point, it is worth mentioning that the XRD patterns of the ZIF-8 membranes after the both post-treatments (i.e., (1) 1st polishing and (2) 2nd time synthesis and polishing) were well-preserved, with being comparable to those of imperfect ZIF-8 membranes and ZIF-8 seeds. This indicates that the main ZIF-8 structure in the membrane was well maintained, while removing or reducing defective structures, originally present in the imperfect ZIF-8 membranes, through the post-treatments.

3.2. Mixture gas permeation

The mixture gas permeation of a ZIF-8 membrane after the 2nd synthesis and polishing was examined at different temperatures with a mixture gas of 50 vol% H_2, 25 vol% CO_2, and 25 vol% CO, which was chosen as a simulated biomass-derived syngas composition without water vapor. As shown in Fig. 5a, the mixture gas permeances of H_2, CO_2, and CO at 30 °C through the ZIF-8 membrane were 13.6×10^{-8}, 4.31×10^{-8}, and 2.89×10^{-8} mol·m^{-2}·s^{-1}·Pa^{-1}, respectively. These permeation values were decreased 30% for H_2 and CO_2 but slightly increased for CO as

12

compared to the single gas permeation results (Table 1). Therefore, the corresponding H_2/CO_2 and H_2/CO separation factors 30 °C were 3.05 and 4.53, respectively, which were lower than the ideal selectivities of 4.47 and 7.57, respectively, as a similar trend was reported by Pan et al [33]. The gas permeation variation in the mixture gas can be attributed to 1) competitive adsorption and diffusion when different gases exist in the membrane system and 2) the concentration polarization impact on the feed side of the membrane. As the temperature increased, the gas permeances further decreased for all gases with the lowest degree of reduction for H_2. Therefore, the separation factors of H_2/CO_2 and H_2/CO increased monotonically with temperature. Specifically, the H_2 permeance at 200 °C decreased approximately 20%, whereas the CO and CO_2 permeances decreased over 50% compared to their permeances at 30 °C. As a result, the corresponding separation factors increased from 3.05 to 5.14 for H_2/CO_2 and from 4.53 to 6.38 H_2/CO. The temperature-dependent gas permeation performance could be explained by the competition between activated diffusion and reduced adsorption with increased temperature [38]. In our case, the gas permeation was primarily in the adsorption-controlled regime, which resulted in the reduction of gas permeances as the temperature increased, especially for the strong adsorption gases CO and CO_2. Though undesirable, we cannot exclude the presence of Knudsen diffusion through the defects in the ZIF-8 membrane, which in turn contributed to decreasing the gas permeances in a partial way.

In a practical syngas environment, water vapor co-exists with the above dry syngas and thus, will affect the gas permeation performance of the ZIF-8 membrane. Here, the mixture gas permeation performance was further investigated under the simulated biomass-derived syngas environment with the presence of 10 vol% steam, as temperature was increased up to 200 °C.

13

The resulting permeation data (Fig. 5b) indicate that the gas permeance of H_2 was almost constant with temperature, while those of CO_2 and CO decreased monotonically with temperatures, as similar to the permeances in the absence of steam (Fig. 5a). The lower gas permeances of all the gases than the counterparts under the dry syngas stream can be ascribed to the condensation and occupation of water molecules in the pore aperture of the ZIF-8 structure, impeding the gas permeation through the ZIF-8 membrane. Nevertheless, the degree of reduction in the gas permeances was not significant for all gases, apparently because of the hydrophobicity of ZIF-8 materials. Specifically, the H_2/CO_2 and H_2/CO separation factors of 4.95 and 6.08 at 200 °C were almost close to 5.14 and 6.38, respectively, obtained under the dry syngas stream (Fig. 5a). As 200 °C is the maximum temperature considered in this study and a higher temperature is desirable for energy-saving H_2 separations from the syngas stream, the weak adsorption of water at high temperatures is beneficial for preserving the performance of ZIF-8 membranes for reliable H_2 separations, regardless of the presence of water in the feed.

3.3. Hydrothermal stability of the ZIF-8 membrane

A hydrothermal stability often prohibits many membranes (e.g., silica membranes and polymeric membranes) from being employed in syngas separation applications with the presence of steam. Although the ZIF-8 membrane shows a potential to separate H_2 from CO and CO_2 (Fig. 5) and ZIF-8 is known as a thermally stable material, to the best of our knowledge, the hydrothermal stability of the ZIF-8 membrane has not been reported under the practical humid syngas environment. As mentioned above, the high hydrothermal stability of ZIF-8s is a key factor to ensure robust H_2 separations. Therefore, we investigated the thermal stability of ZIF-8

particles under various gaseous environments and found that the ZIF-8 structure was least stable under a steam atmosphere [48]. Although similar H_2 perm-selectivities that indicate the preferred permeation of H_2 over other gases were observed in both dry and wet conditions at 200 °C, it is necessary to confirm the applicability of the ZIF-8 membrane for reliable H_2 separations from biomass-derived syngas. To this end, the hydrothermal stability was examined by observing the performance of the ZIF-8 membrane under the simulated syngas environment with the presence of 10 vol% steam at 200 °C. As shown in Fig. 6, the gas permeances and separation factors were not significantly changed up to ~10 h. However, all the gas permeances started to increase slowly after 10 h and concomitantly, the separation factors were decreased. After 15 h, the H_2 permeance increased by more than 75% and the CO and CO_2 permeances were increased to almost 2 times of their initial permeances, resulting in the H_2/CO_2 and H_2/CO separation factors being lowered to 3.32 and 3.59, respectively. The performance variation indicated that the ZIF-8 membrane have a limitation for membrane-based H_2 separations as it started to lose its molecular sieve functionality after 10 h at 200 °C under the simulated biomass-derived syngas environment with the presence of 10 vol% steam. In addition, the single gas permeation test was conducted at room temperature by using the ZIF-8 membrane after the hydrothermal stability test. The gas permeances of H_2, CO, and CO_2 were $35.13×10^{-8}$, $14.56×10^{-8}$ and $10.26×10^{-8}$ mol·m^{-2}·s^{-1}·Pa^{-1} with the corresponding H_2/CO_2 and H_2/CO ideal selectivities of 3.42 and 2.41, respectively. These ideal selectivities were very close to the single gas permeation results of the imperfect ZIF-8 membrane (3.03 and 2.49 in Table 1). Therefore, one may conclude that the ZIF-8 membrane is not able to serve as the H_2-selective membranes for a long-term purpose, since its exposure to the steam-containing syngas environment at 200 °C for 15 h resulted in deteriorating the separation performance eventually toward that of the bare supports.

15

The XRD patterns of the ZIF-8 membranes after the hydrothermal stability test were consistent with the simulated ZIF-8 pattern (Fig. 7), indicating the ZIF-8 structure was still preserved in spite of the lowered H_2 separation performance. Along with the XRD patterns shown in Fig. 4, this result suggests that the XRD analysis should be complemented with the permeation measurement to draw a proper conclusion relevant to the separation performance of ZIF-8 membranes. As expected, the hydrothermal exposure led to irregular-shaped ZIF-8 grains and cracks on the top surface of the ZIF-8 membranes as shown in the SEM image (Fig. 8a). Fig. 8b shows that the membrane thickness of the ZIF-8 membrane was slightly decreased after the hydrothermal stability test. Unfortunately, all these results were consistent with our findings on the thermal stability of ZIF-8 particles [48]. Specifically, the particles with the ZIF-8 structure could be maintained at a temperature lower than 300 °C for 5 h under steam conditions with some loss of its crystallinity, though ZIF-8 structures were well preserved at the same temperature under inert argon conditions. Considering both the crystallinity and defect are critical for preserving the separation performance of a ZIF-8 membrane, deliberate choices for the reliable use through ZIF-8 membranes should be satisfied; inert conditions will be much beneficial for utilizing the H_2 separation performance of ZIF-8 membranes.

Based on the hydrothermal stability test, we conclude that the ZIF-8 membrane is not suitable for long-term H_2 separations in the biomass-derived syngas environment with the presence of steam at temperatures over 200 °C. Similarly, ZIF-8 membrane applications in the water gas shift reaction and other steam-involved reactions at temperatures of over 200 °C are practically inappropriate. This directs to the need of additional post-treatments that allow for

overcoming the low hydrothermal stability of ZIF-8 membranes for their realization in real applications. At the same time, new approaches need to be developed in order to preserve the H_2 separation performance of intact ZIF-8 membranes.

4. Conclusions

In this study, a zeolitic imidazolate framework-8 (ZIF-8) membrane was successfully prepared with well-developed post-treatment methods. The proposed post-treatment methods, including (1) a polishing and (2) a 2nd time synthesis followed by polishing, repaired imperfect ZIF-8 membranes and thus, improved the reliability of ZIF-8 membrane fabrications. The gas separation performance of the post-treated ZIF-8 membrane was examined by single gas permeation at room temperature and subsequently, mixture gas permeation at different temperatures in a simulated biomass-derived syngas environment with and without the presence of steam. The results demonstrated that the treated ZIF-8 membrane had a modest performance for H_2 separations (H_2/CO_2 and H_2/CO separation factor of 5.14 and 6.38 at 200 °C, respectively) in the simulated environments and the presence of water vapor reduced the permeation rates of all the gases with the similar H_2/CO_2 and H_2/CO separation factors (4.95 and 6.08 at 200 °C, respectively). Finally, the hydrothermal stability of the ZIF-8 membrane was investigated in simulated humid biomass-derived syngas environments. Despite the promise for H_2 separation from CO and CO_2 in the absence and presence of water in the feed, the poor hydrothermal stability limits the application of ZIF-8 membranes for long-term H_2 separations in biomass-derived syngas environments over 200 °C. Currently, we are making an effort to propose new

17

approaches that lead to preserving the H_2 perm-selectivity of ZIF-8 membranes under steam-containing feeds at temperatures higher than 200 °C.

Acknowledgements

Reference

[1] J. Hongrapipat, W.L. Saw, S. Pang, Fuel 139, (2015) 494-501.

[2] J.A. Ruiz, M.C. Juarez, M.P. Morales, P. Munoz, M.A. Mendivil, Renew. Sust. Energ. Rev. 18, (2013) 174-183.

[3] W. Saw, H. McKinnon, I. Gilmour, S.S. Pang, Fuel 93, (2012) 473-478.

[4] W.L. Saw, S.S. Pang, Fuel 112, (2013) 117-124.

[5] J. Hongrapipat, W. Saw, S. Pang, Biomass Conv. Bioref. 2, (2012) 327-348.

[6] K. Kumabe, T. Hanaoka, S. Fujimoto, T. Minowa, K. Sakanishi, Fuel 86, (2007) 684-689.

[7] M. Packer, Energy Policy 37, (2009) 3428-3437.

[8] S. Pang, J. Li, New. Zeal. J. For. 51, (2006) 7-12.

[9] E.E. McLeary, J.C. Jansen, F. Kapteijn, Microporous Mesoporous Mat. 90, (2006) 198-220.

[10] T. Yang, T.S. Chung, Int. J. Hydrog. Energy 38, (2013) 229-239.

[11] S.L. James, Chem. Soc. Rev. 32, (2003) 276-288.

[12] H. Li, M. Eddaoudi, M. O'Keeffe, O.M. Yaghi, Nature 402, (1999) 276-279.

[13] S.T. Meek, J.A. Greathouse, M.D. Allendorf, Adv. Mater. 23, (2011) 249-267.

[14] K.S. Park, Z. Ni, A.P. Cote, J.Y. Choi, R.D. Huang, F.J. Uribe-Romo, H.K. Chae, M. O'Keeffe, O.M. Yaghi, Proc. Natl. Acad. Sci. U. S. A. 103, (2006) 10186-10191.

[15] J.L.C. Rowsell, O.M. Yaghi, Microporous Mesoporous Mat. 73, (2004) 3-14.

[16] H.C. Zhou, J.R. Long, O.M. Yaghi, Chem. Rev. 112, (2012) 673-674.

[17] J. Cravillon, S. Munzer, S.J. Lohmeier, A. Feldhoff, K. Huber, M. Wiebcke, Chem. Mater. 21, (2009) 1410-1412.

[18] J. Cravillon, R. Nayuk, S. Springer, A. Feldhoff, K. Huber, M. Wiebcke, Chem. Mater. 23, (2011) 2130-2141.

[19] J. Cravillon, C.A. Schroder, H. Bux, A. Rothkirch, J. Caro, M. Wiebcke, Crystengcomm 14, (2012) 492-498.

[20] X.C. Huang, Y.Y. Lin, J.P. Zhang, X.M. Chen, Angew. Chem.-Int. Edit. 45, (2006) 1557-1559.

[21] Y.C. Pan, Y.Y. Liu, G.F. Zeng, L. Zhao, Z.P. Lai, Chem. Commun. 47, (2011) 2071-2073.

[22] B.R. Pimentel, A. Parulkar, E.K. Zhou, N.A. Brunelli, R.P. Lively, Chemsuschem 7, (2014) 3202-3240.

[23] Y.Q. Tian, C.X. Cai, Y. Ji, X.Z. You, S.M. Peng, G.H. Lee, Angew. Chem.-Int. Edit. 41, (2002) 1384-1386.

[24] H. Bux, F.Y. Liang, Y.S. Li, J. Cravillon, M. Wiebcke, J. Caro, J. Am. Chem. Soc. 131, (2009) 16000-16001.

[25] X.L. Liu, H. Jin, Y.S. Li, H. Bux, Z.Y. Hu, Y.J. Ban, W.S. Yang, J. Membr. Sci. 428, (2013) 498-506.

[26] M.C. McCarthy, V. Varela-Guerrero, G.V. Barnett, H.K. Jeong, Langmuir 26, (2010) 14636-14641.

[27] A. Corma, H. Garcia, F. Xamena, Chem. Rev. 110, (2010) 4606-4655.

[28] J. Lee, O.K. Farha, J. Roberts, K.A. Scheidt, S.T. Nguyen, J.T. Hupp, Chem. Soc. Rev. 38, (2009) 1450-1459.

[29] J.W. Liu, L.F. Chen, H. Cui, J.Y. Zhang, L. Zhang, C.Y. Su, Chem. Soc. Rev. 43, (2014) 6011-6061.

[30] H. Yin, J. Choi, A.C.K. Yip, Catal. Today, (2015) http://dx.doi.org/10.1016/j.cattod.2015.08.030.

[31] P. Horcajada, C. Serre, G. Maurin, N.A. Ramsahye, F. Balas, M. Vallet-Regi, M. Sebban, F. Taulelle, G. Ferey, J. Am. Chem. Soc. 130, (2008) 6774-6780.

[32] Y.S. Li, F.Y. Liang, H.G. Bux, W.S. Yang, J. Caro, J. Membr. Sci. 354, (2010) 48-54.

[33] Y.C. Pan, B. Wang, Z.P. Lai, J. Membr. Sci. 421, (2012) 292-298.

[34] M. Shah, H.T. Kwon, V. Tran, S. Sachdeva, H.K. Jeong, Microporous Mesoporous Mat. 165, (2013) 63-69.

[35] K. Tao, C.L. Kong, L. Chen, Chem. Eng. J. 220, (2013) 1-5.

[36] J.F. Yao, L.X. Li, W.H.B. Wong, C.Z. Tan, D.H. Dong, H.T. Wang, Mater. Chem. Phys. 139, (2013) 1003-1008.

[37] H.L. Huang, W.J. Zhang, D.H. Liu, B. Liu, G.J. Chen, C.L. Zhong, Chem. Eng. Sci. 66, (2011) 6297-6305.

[38] Y.C. Pan, T. Li, G. Lestari, Z.P. Lai, J. Membr. Sci. 390, (2012) 93-98.

[39] H.T. Kwon, H.K. Jeong, J. Am. Chem. Soc. 135, (2013) 10763-10768.

[40] A.S. Huang, Q. Liu, N.Y. Wang, J. Caro, Microporous Mesoporous Mat. 192, (2014) 18-22.

[41] D.W. Breck, *Zeolite Molecular Sieves: Structure, Chemistry, and Use*. 1974: John Wiley & Sons, Inc.

[42] G.S. Xu, J.F. Yao, K. Wang, L. He, P.A. Webley, C.S. Chen, H.T. Wang, J. Membr. Sci. 385, (2011) 187-193.

[43] R. Krishna, J.M. van Baten, J. Membr. Sci. 360, (2010) 323-333.

[44] H. Bux, A. Feldhoff, J. Cravillon, M. Wiebcke, Y.S. Li, J. Caro, Chem. Mater. 23, (2011) 2262-2269.

[45] J.F. Yao, D.H. Dong, D. Li, L. He, G.S. Xu, H.T. Wang, Chem. Commun. 47, (2011) 2559-2561.

[46] V.M.A. Melgar, J. Kim, M.R. Othman, J. Ind. Eng. Chem. 28, (2015) 1-15.

[47] K. Keizer, R.J.R. Uhlhorn, R.J. Vanvuren, A.J. Burggraaf, J. Membr. Sci. 39, (1988) 285-300.

[48] H. Yin, H. Kim, J. Choi, A.C.K. Yip, Chem. Eng. J. 278, (2015) 293-300.

Table 1. Single gas permeances of the support and synthesized membranes at room temperature.

Samples	Pure Gas Permeance (10^{-8} mol / $m^2 \cdot s \cdot Pa$)				Pure Gas Selectivity Factor		
	H_2	CO_2	CO	N_2	H_2 / CO_2	H_2 / N_2	H_2 / CO
Support	1150	317	375	381	3.63	3.02	3.08
Imperfect Membrane	62.4	20.6	4.28	4.63	3.03	2.59	2.49
Post-treatment (1st Polishing)	20.5	4.28	2.31	1.57	4.79	13.06	8.87
Post-treatment (2nd synthesis + Polishing)	20.8	4.63	2.74	1.54	4.47	13.35	7.57
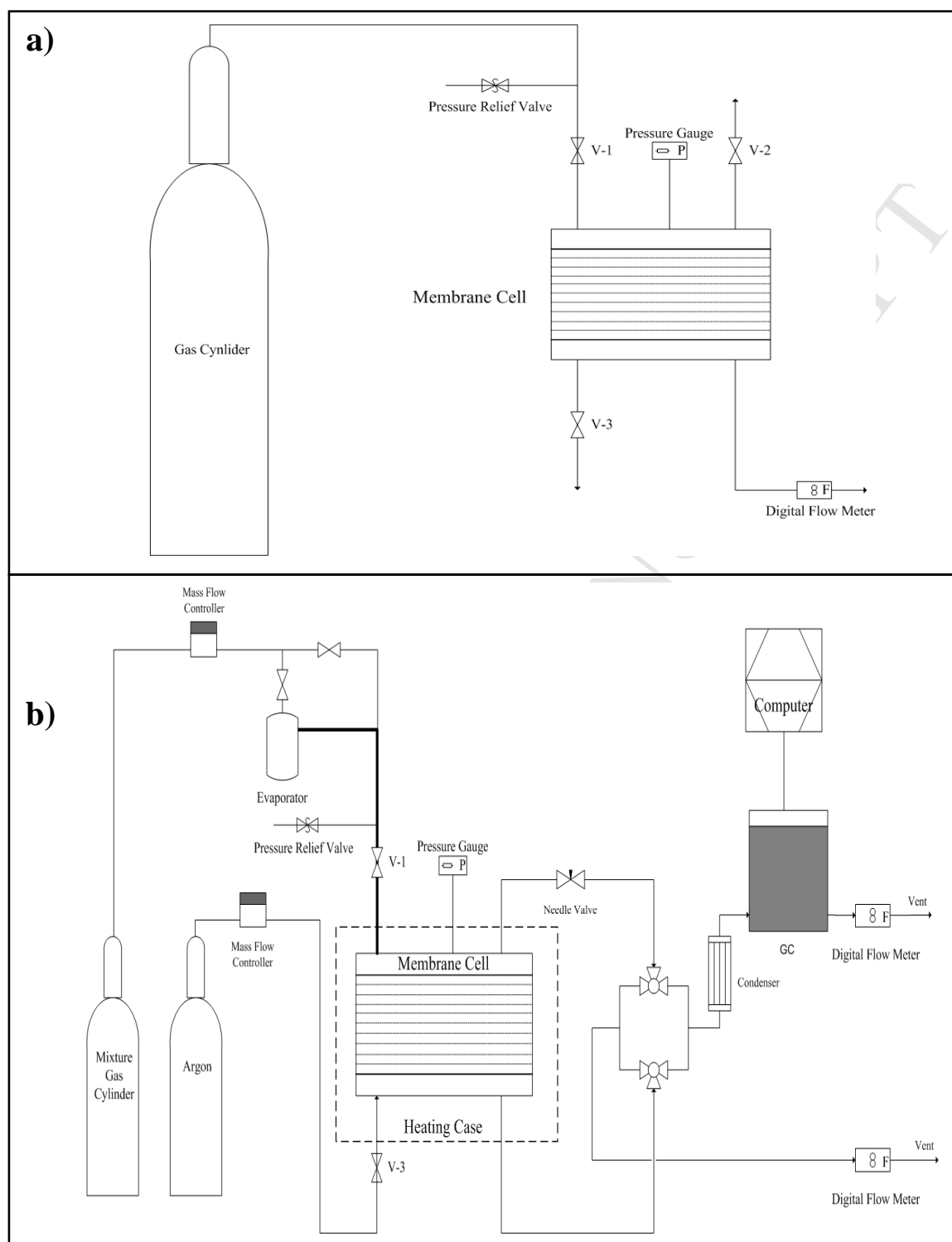
**Fig. 1.** Schematic diagram of the gas permeation setup for (a) single gases and (b) mixture gases.
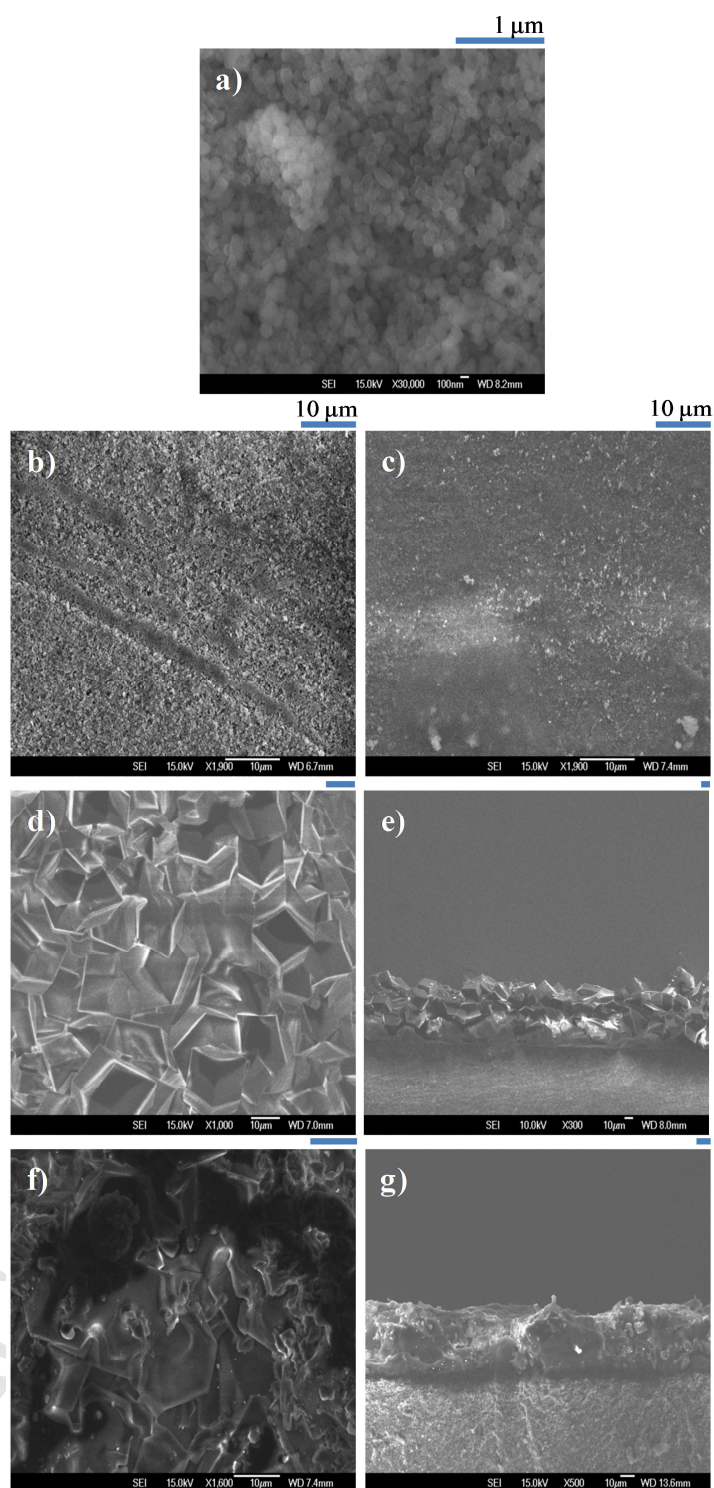
Fig. 2. SEM images of (a) ZIF-8 seeds, (b) bare α-alumina support, (c) seeded support, (d) top surface and (e) cross-section of the dried ZIF-8 membrane, (f) top surface and (g) cross-section of a 1st polished ZIF-8 membrane.
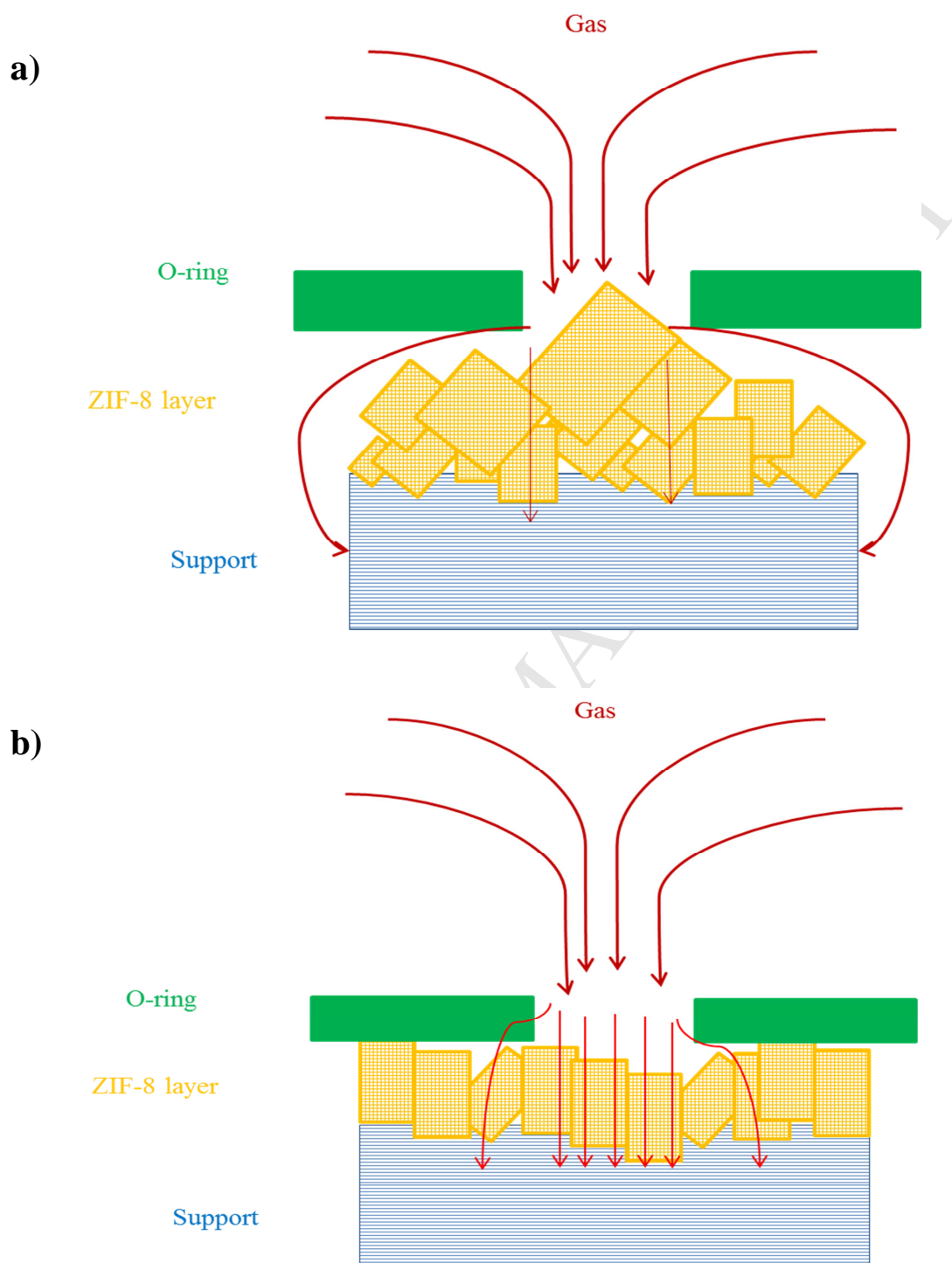
Fig. 3. Schematic diagrams of gas permeation pathways through the membrane (a) before and (b) after the polishing post-treatment.
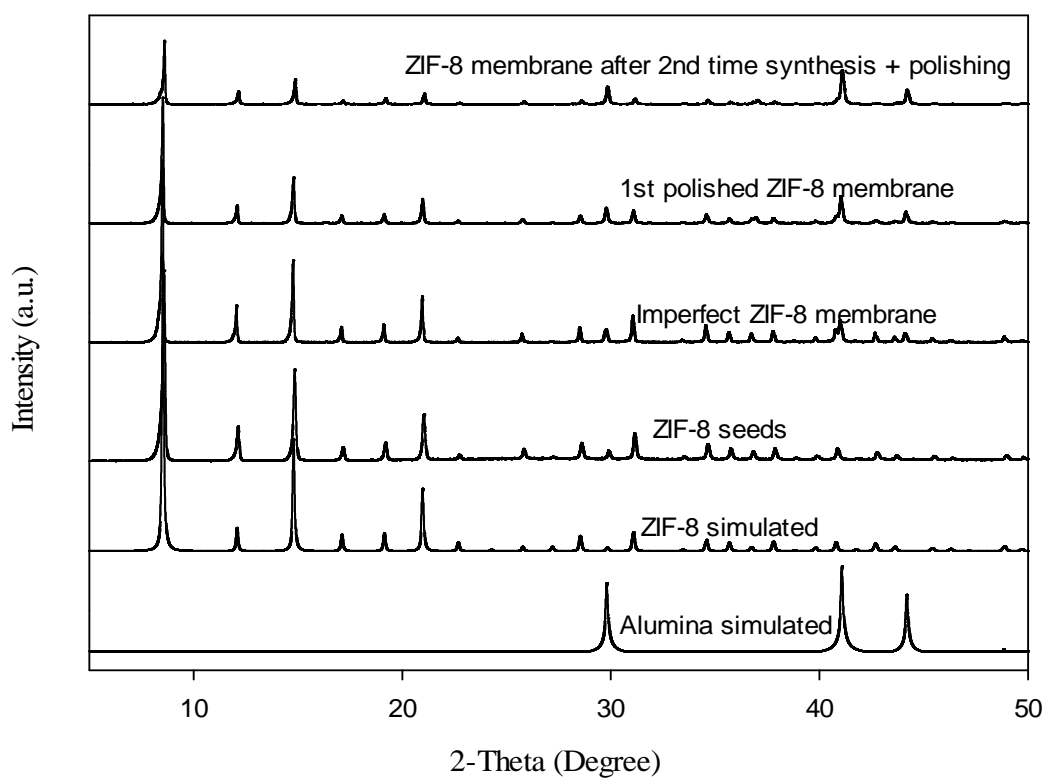
Fig. 4. XRD patterns of the ZIF-8 seeds, the imperfect ZIF-8 membrane, the 1st polished ZIF-8 membrane, and the ZIF-8 membrane after the 2nd synthesis and polishing. For comparison, the simulated XRD patterns of ZIF-8 and α-alumina are included.

25
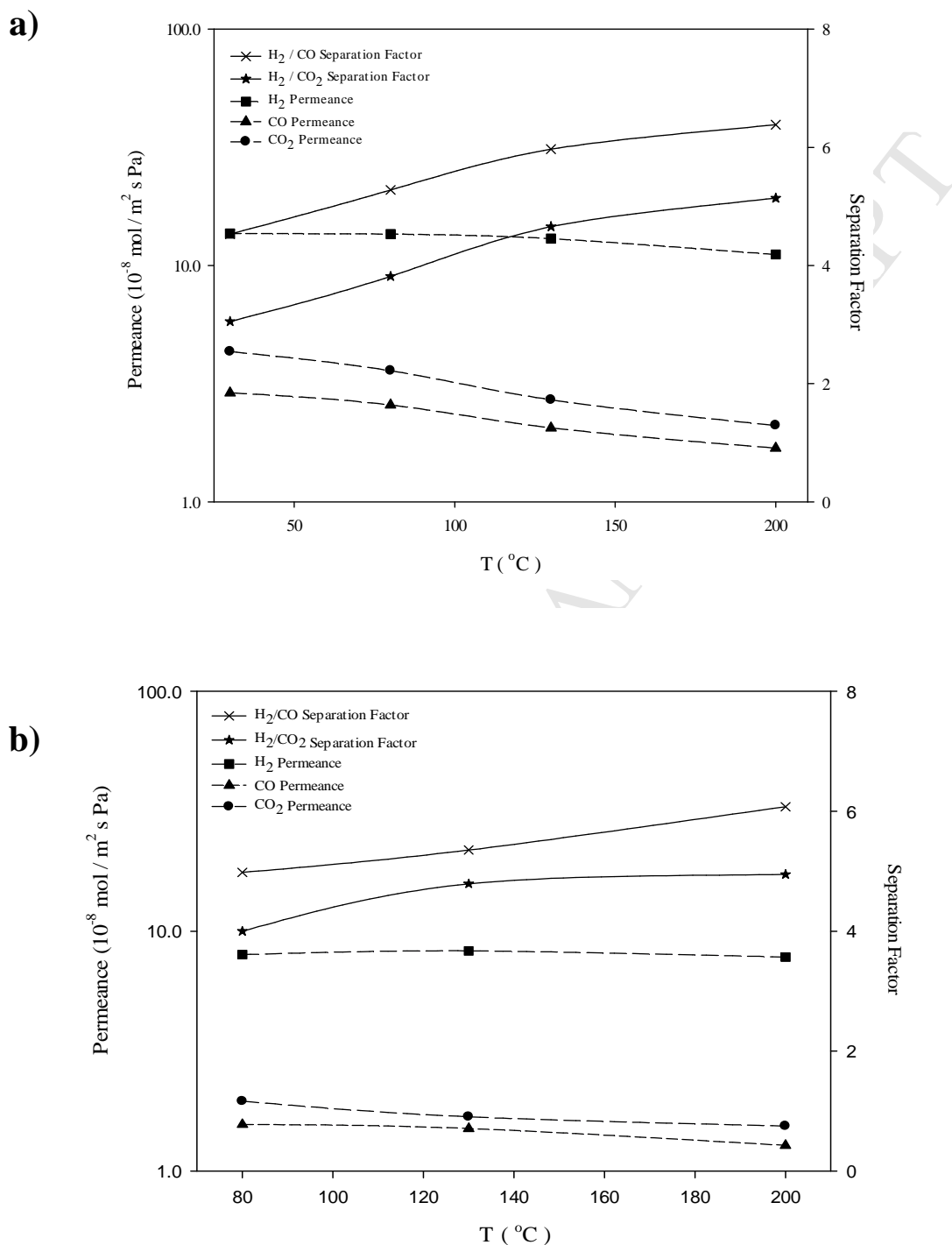
**Fig. 5.** Permeances of H_2, CO_2, and CO and the corresponding H_2/CO_2 and H_2/CO separation factors through a ZIF-8 membrane (obtained by a 2nd time synthesis and polishing) at different temperatures (a) without and (b) with the presence of 10 vol% steam.
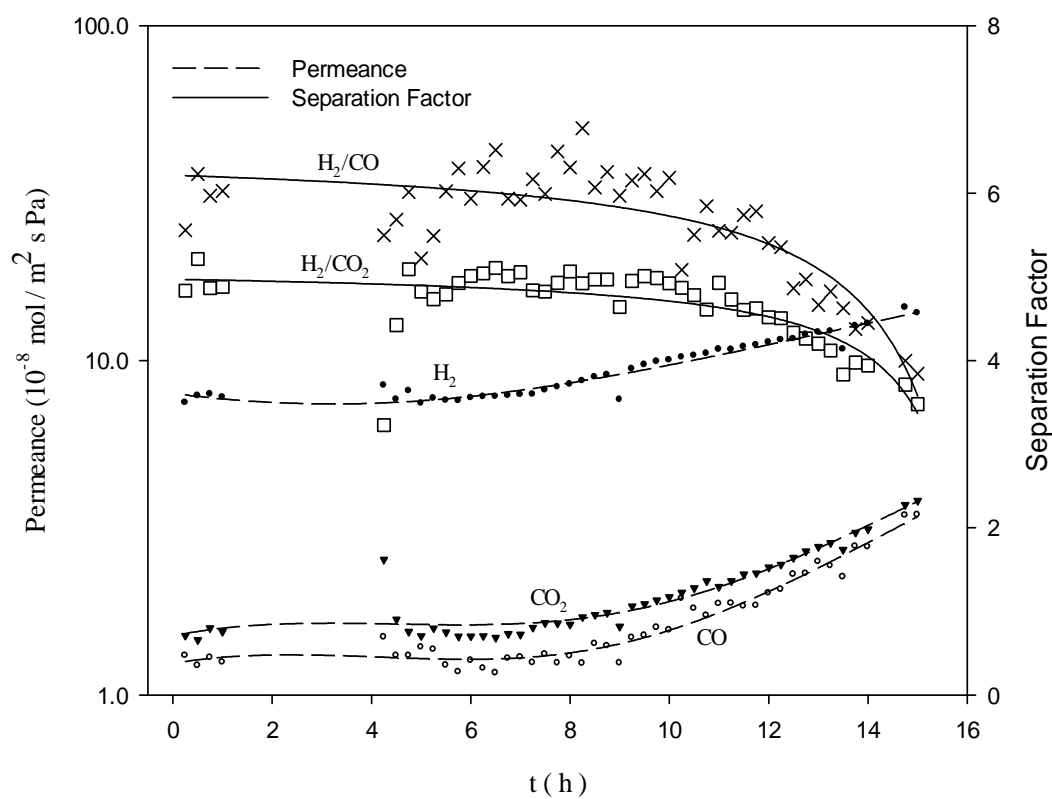
Fig. 6. Long-term gas permeances of H_2, CO_2, and CO and the corresponding H_2/CO_2 and H_2/CO separation factors through the ZIF-8 membrane (obtained by a 2nd time synthesis and polishing) at 200 °C under the 10 vol% steam.
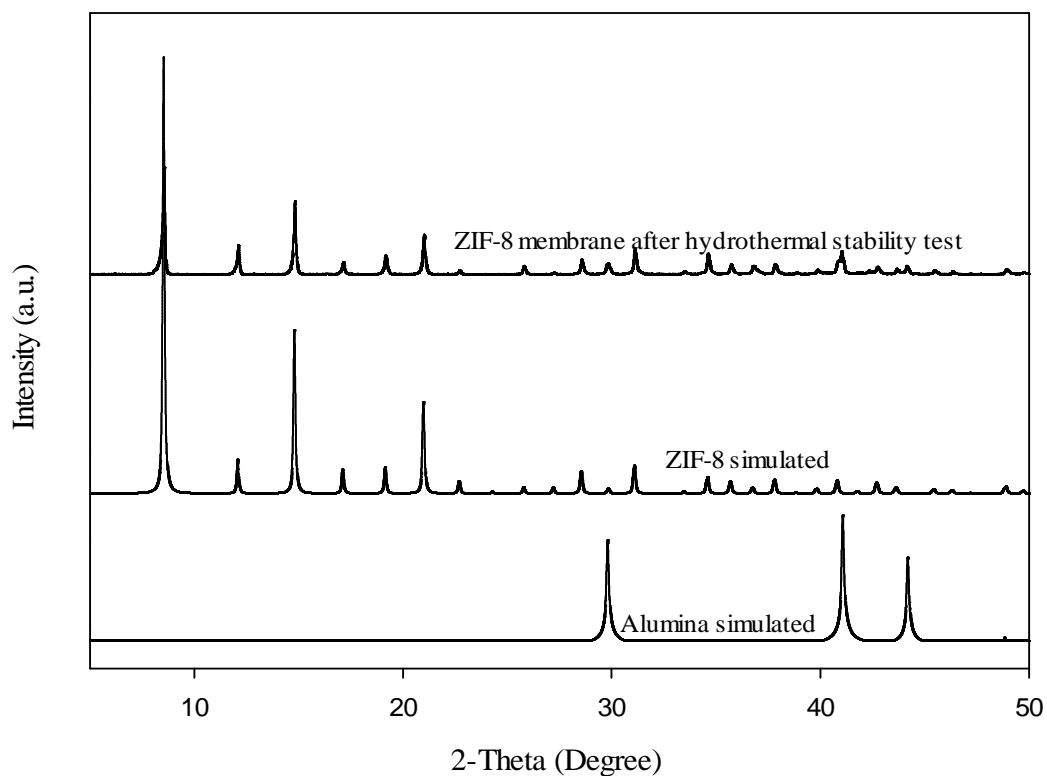
Fig. 7. XRD pattern of the ZIF-8 membrane (obtained by a 2nd time synthesis and polishing) used for the hydrothermal stability test at 200 °C for 15 h. For comparison, the simulated XRD patterns of ZIF-8 and α-alumina are included.
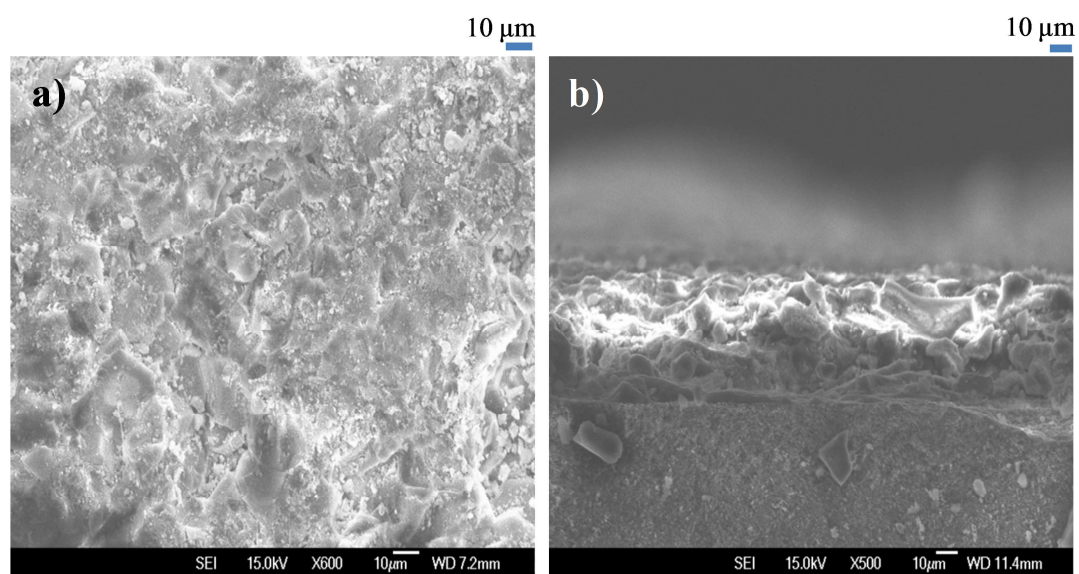
Fig. 8. SEM images of (a) the top surface and (b) cross-section of the ZIF-8 membrane (obtained by a 2nd time synthesis and polishing) used for the hydrothermal stability test at 200 °C for 15 h.

Highlights

- ZIF-8 membranes were successfully prepared with post-treatments.

- ZIF-8 membranes gave good H_2 separation performance in a simulated syngas environment.

- The hydrothermal stability of the ZIF-8 membrane was evaluated.